

Instabilities and Chaos in Optics

F. T. Arecchi

Istituto Nazionale di Ottica and Dept. of Physics, University of Firenze, Italy

Received August 14, 1987; accepted November 30, 1987

Abstract

The onset of deterministic chaos in lasers is studied by referring to low dimensional systems, in order to isolate the characteristics of chaos from the random fluctuations due to the coupling with a thermal reservoir. For this purpose, attention is focused on single mode homogeneous line lasers, whose dynamics is ruled by a low number of coupled variables. In the examined cases, experiments and theoretical model are in close agreement. In particular I describe Shilnikov chaos, how it can be characterized, and the strong resulting coupling between nonlinear dynamics and statistical mechanics.

1. Coherence and chaos in lasers

Quantum optics from its beginning was considered as the physics of coherent and intrinsically stable radiation sources. Lamb's semiclassical theory [1] showed the role of the e.m. field in the cavity in ordering the phases of the induced atomic dipoles, thus giving rise to a macroscopic polarization and making it possible a description in terms of very few collective variables. In the case of a single mode laser and a homogeneous gain line this means just five coupled degrees of freedom, namely, a complex field amplitude E , a complex polarization P , and a population inversion N . A corresponding quantum theory, even for the simplest laser model, does not lead to a closed set of equations, however the interaction with other degrees of freedom acting as a thermal bath (atomic collisions, thermal radiation) provides truncation of high order terms in the atom-field interaction [2–4]. The problem may be reduced to five coupled equations (the so-called Maxwell Bloch equations) but now they are affected by noise sources to account for the coupling with the thermal bath [5]. Being stochastic, or Langevin, equations, the corresponding solution in closed form refers to a suitable weight function or phase space density. Anyway the average motion matches the semiclassical one, and fluctuations play a negligible role if one excludes the bifurcation points where there are changes of stability in the stationary branches. Leaving out the peculiar statistical phenomena which characterize the threshold points and which suggested a formal analogy with thermodynamic phase transitions [6] the main point of interest is that a single mode laser provides a highly stable or coherent radiation field.

From the point of view of the associated information, the standard interferometric or spectroscopic measurements of classical optics, relying on average field values or on their first order correlation functions, are insufficient. In order to characterize the statistical features of Quantum optics it was necessary to make extensive use of photon statistics [7, 8].

From a dynamical point of view, coherence is equivalent of having a stable fixed point attractor and this does not depend on details of the nonlinear coupling, but on the number of relevant degrees of freedom. Since such a number depends on the time scales on which the output field is

observed, coherence becomes a question of time scales. This is the reason why for some lasers coherence is a robust quality, persistent even in presence of strong perturbations, whereas in other cases coherence is easily destroyed by the manipulations common in the laboratory use of lasers, such as modulation, feedback or injection from another laser.

Here I give a general presentation of low dimensional chaos in lasers. For a more complete approach to the problem, I refer to a recent monograph on the subject [9].

We focus on those situations in quantum optics which permit close comparison between experiments and theory. By purpose I do not tackle the vast class of inhomogeneously broadened lasers, where it is extremely difficult to derive close correspondences between experiments and theory because of the large number of coupled degrees of freedom.

If we couple Maxwell equations with Schrödinger equations for N atoms confined in a cavity, and expand the field in cavity modes, keeping only the first mode which goes unstable, this is coupled with the collective variables P and Δ describing the atomic polarization and population inversion as follows (E being the slowly varying mode amplitude)

$$\begin{aligned} \dot{E} &= -kE + gP, \\ \dot{P} &= -\gamma_{\perp}P + g\Delta E, \\ \dot{\Delta} &= -\gamma_{\parallel}(\Delta - \Delta_0) - 4gPE. \end{aligned} \quad (1)$$

For simplicity we consider the cavity frequency at resonance with the atomic resonance, so that we can take E and P as real variables and we have three coupled equations. Here, k , γ_{\perp} , γ_{\parallel} are the loss rates for field, polarization and population respectively, g is a coupling constant and Δ_0 is the population inversion which would be established by the pump mechanism in the atomic medium, in the absence of coupling. While the first equation comes from Maxwell equations, the other two imply the reduction of each atom to a two-level atom resonantly coupled with the field.

The presence of loss rates means that the three relevant degrees of freedom are in contact with a "sea" of other degrees of freedom. In principle eqs. (1) could be deduced from microscopic equations by statistical reduction techniques [5].

The similarity of Maxwell–Bloch equations (1) with Lorenz equations [10] would suggest the easy appearance of chaotic instabilities in single-mode, homogeneous-line lasers. Indeed Lorenz model is a suggestive example of the general fact that a nonlinear coupling of at least three dynamical degree of freedom may induce instabilities on the motion, which in such cases becomes irregular. However time scale considerations rule out the full dynamics for most of the available lessers. Lorenz equations have damping rates within one order of magnitude. On the contrary, in most lasers the three damping rates are wildly different from one another.

The following classification has been introduced [11]

Class A (e.g., He-Ne, Ar, Kr, dye): $\gamma_{\perp} \simeq \gamma_{\parallel} \gg k$.

The two last equations can be solved at equilibrium (adiabatic elimination procedure) and one single nonlinear field equation describes the laser. $N = 1$ means fixed point attractor, hence coherent emission.

Class B (e.g., ruby, Nd, CO₂): $\gamma_{\perp} \gg k \lesssim \gamma_{\parallel}$.

Only polarization is adiabatically eliminated and the dynamics is ruled by two rate equations for field and population. $N = 2$ allows also for period oscillations.

Class C

The complete set of eqs. (1) has to be used, hence Lorenz like chaos is feasible, whenever $\gamma_{\perp} \simeq \gamma_{\parallel} \simeq k$.

We have carried a series of experiments on the birth of deterministic chaos in CO₂ lasers (Class B). In order to increase by at least 1 the number of degrees of freedom, we have tested the following configurations.

(i) Introduction of a time dependent parameter to make the system non autonomous [12]. Precisely, an electro-optical modulator modulates the cavity losses at a frequency near the proper oscillation frequency Ω provided by a linear stability analysis, which for a CO₂ laser happens to lie in the 50–100 KHz range, making it easy an accurate set of measurements.

(ii) Injection of signal from an external laser detuned with respect to main one, choosing the frequency difference near the above mentioned Ω . With respect to the external reference the laser field has two quadrature components which represent two dynamical variables. Hence we reach $N = 3$ and observe chaos [11].

(iii) Use a bidirectional ring, rather than a Fabry-Perot cavity [13]. In the latter case the boundary conditions constrain forward and backward wave, by phase relations on the mirror, to act as a single standing wave. In the former case forward and backward waves have just to fill the total ring length with an interger number of wavelengths but there are no mutual phase constrains, hence they act as two separate variables. Furthermore, when the field frequency is detuned with respect to the center of the gain line, a complex population grating arises from interference of the two counter-going waves, and as a result the dynamics becomes rather complex, requiring $N > 3$ dimensions.

(iv) Add an overall feedback, besides that provided by the cavity mirrors, by modulating the losses with a signal provided by the output intensity [14]. If the feedback has a time constant comparable with the population decay time, it provides a third equation sufficient to yield chaos.

Notice that while methods (i), (ii) and (iv) require an external device, (iii) provides intrinsic chaos. In any case, since feedback, injection or modulation are currently used in laser applications, the evidence of chaotic regions puts a caution on the optimistic trust in the laser coherence.

Of course, the requirement of three coupled nonlinear equations does not necessarily restrict the attention to just Lorenz equations. In fact none of the explored cases (i) to (iv) corresponds to Lorenz chaos.

2. Shil'nikov chaos, the method of return times and the fluctuation enhancement

Of the whole phenomenology explored in the past years, I

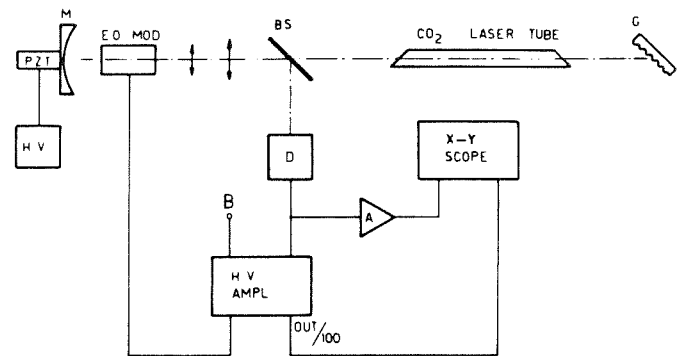


Fig. 1. Experimental set up. M – total reflecting mirror mounted on a PZT drive. E.O.MOD – electro-optic modulator. BS – ZnSe beam splitter. G – grating. D – HgCdTe detector. B – bias voltage.

select a single topic of particular relevance. I report experimental evidence of quasi homoclinic behavior characterized by pulses with regular shapes but chaotic in their time sequence [15]. The regularity in the shape means that the points at any Poincaré section are so closely packed that extremely precise measurements of their position would be required to yield relevant features of the motion. On the contrary, return times to a Poincaré section close to the unstable point display a large spread, due to the sensitive dependence of the motion upon the intersection coordinate. Based on such a consideration, we introduce the spread in return times as the specific indicator of homoclinic chaos. Our experimental data yield iteration maps of return times in close agreement with those arising from the theory of Shil'nikov chaos [16, 17]. Thus, the test introduced in Ref. [15] appears as the most direct one to characterize chaotic dynamical situations associated with pulses almost equal in shape but having fluctuating occurrence times. Furthermore, at variance with the theory, the experimental return maps show a variable degree of thickening independent from the measurement accuracy. This is the phenomenon of fluctuation enhancement already described in the decay of the unstable state of a macroscopic system [18]. This phenomenon introduces unavoidable statistical features in the nonlinear dynamics of a macroscopic system. In such case the collective description in terms of a few dynamical variables breaks down, because of large fluctuations. This was first observed in the switch-on of a laser [18a] and then in many quenching phenomena as spinodal decomposition [18b].

Our experimental evidence of Shil'nikov type instability is based on a quantum optical system, namely a laser with an overall feedback. Precisely, we work on a single mode CO₂ laser with an intracavity electro-optic modulator yielding cavity losses proportional to the laser output intensity (Fig. 1) [14]. In an appropriate range of the control parameters, the dynamical behavior consists of closed orbits visiting successively the neighbourhoods of three unstable stationary points, one of which is a saddle focus [19]. The points are embedded in a three dimensional phase space [14], hence they have three eigenvectors each (Figs. 2 and 3) Ref. [19] describes the competition of the three instabilities in controlling the global features of the motion. We adjust the control parameter in order to have a dominance of the saddle focus and reduce the influence of the other two instabilities. This way, the motion consists of a homoclinic orbit asymptotic to the saddle focus. This instability provides an exponential

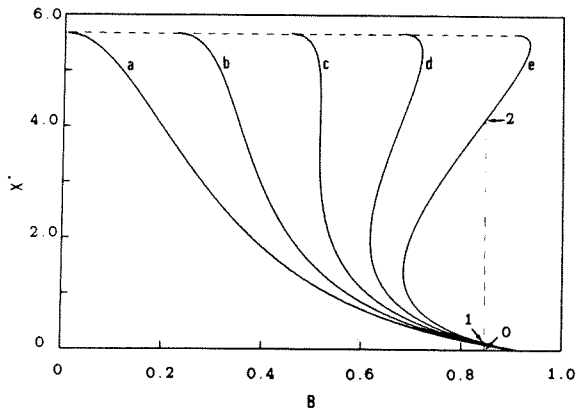


Fig. 2. Plot of the normalized stationary intensity x^* versus B for a given pump rate. Call r the gain of the feedback loop. Curves (a), (b), (c), (d) and (e) refer to $r = 0.0, 0.04, 0.08, 0.12$ and 0.16 respectively. Points 0, 1 and 2 indicated by arrows, are the stationary points for $B = 0.838$ and $r = 0.16$.

divergence within the flow while the homoclinic orbit ensures that at least a portion of this diverging flow is reinjected into the neighbourhood of the saddle focus. This structure of the flow is one of the simplest capable of generating chaotic behaviour in many autonomous systems like for instance the Lorenz equations [20] or the Belousov-Zhabotinskii reaction [21]. The figures show clear evidence of a homoclinic orbit with long transients, which provide a lengthy permanence in a phase space region of almost constant intensity. This appears more clearly in the corresponding phase space projections (Figs. 4 and 5).

We measure the time spacing between successive orbits by setting a threshold circuit near the top of the largest peak of the intensity signal. A time to amplitude converter yields the sequence τ_i of successive time spacings, which is then classified as a statistical distribution by a multichannel pulse height analyser, or stored in a digitizer, so that correlation functions or return maps can be sorted out.

The statistical distribution of return times is a broad featureless curve which does not offer clues on the ordering of τ_i . On the contrary, the return map displays an extremely regular structure (Fig. 6). To check whether we are in presence of a one dimensional (1D) return map and the remaining thickness is due to the observation technique, or

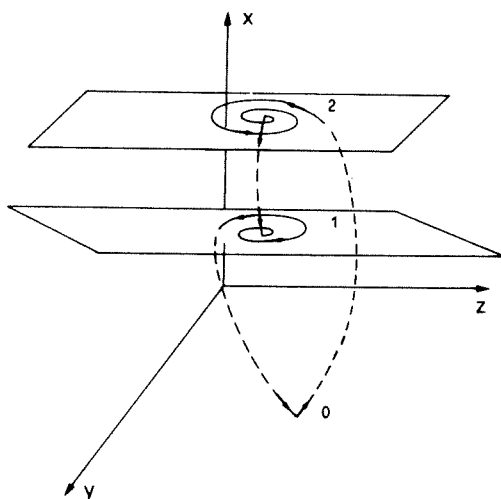


Fig. 3. Schematic view of a trajectory in the phase space (x = laser intensity, y = population inversion, z = feedback voltage) when the dynamics is affected by all the three unstable stationary points.

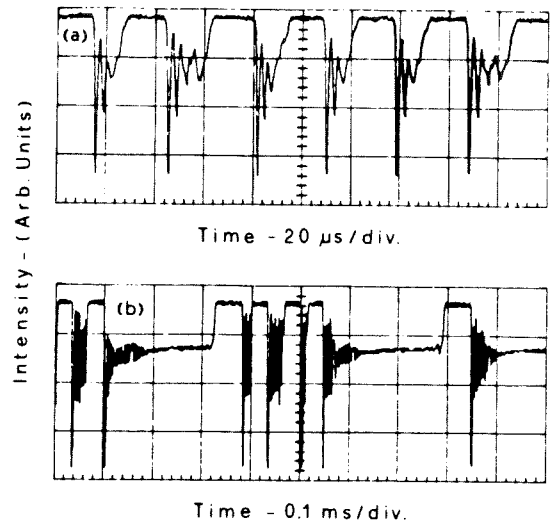


Fig. 4. Time plots of the laser intensity $x(t)$ in the regime of Shil'nikov chaos. Intensity increases downward. (a) and (b) refer to the same B value, but two different gain r of the feedback loop. (b) shows two long transients corresponding to a large number of small spirals around the saddle focus [see also Fig. 5(b)].

the map is more than 1D and its thickness hides new information, we measure also the return maps corresponding to three regular periodic situations. In the absence of fluctuations in τ_i they should be point like. In fact (1) corresponds to an electronic oscillator and it just shown the resolution of the measurement, (2) corresponds to the laser in a regular periodic regime away from the Shil'mikov instability, and (3) corresponds to the laser just on the verge of the instability but still with a regular period. In this last case, the fluctuation associated with the nearby transition shows that, even without chaos in the return time, the close approach to an instability point introduces a fluctuation enhancement, which has no theoretical counterpart in the current treatment of deterministic chaos.

To deal with this broadening, the dynamical equations should include a statistical spread in the injection coordinate to account for the macroscopic character of the experimental system (Fig. 7). As it was shown in Ref. [18], even though this

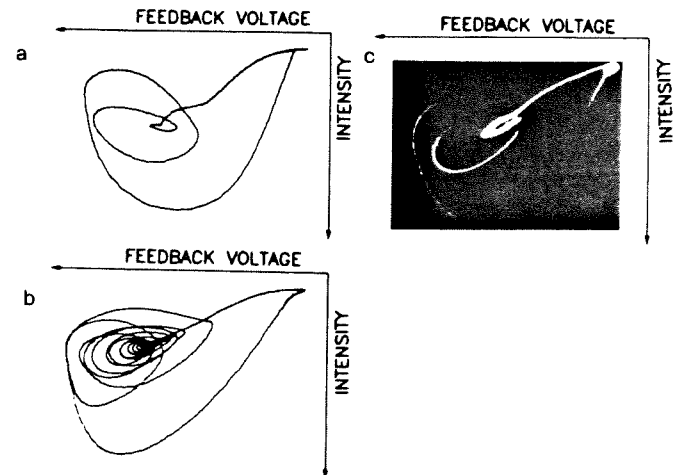


Fig. 5. Phase space projections x - z (laser intensity-feedback voltage). (a) and (b) are single orbits obtained by a digitizer, while (c) is a photographic exposure over 1 sec. (a) and (b) refer respectively to the same parameter situation of Fig. 4(a) and (b).

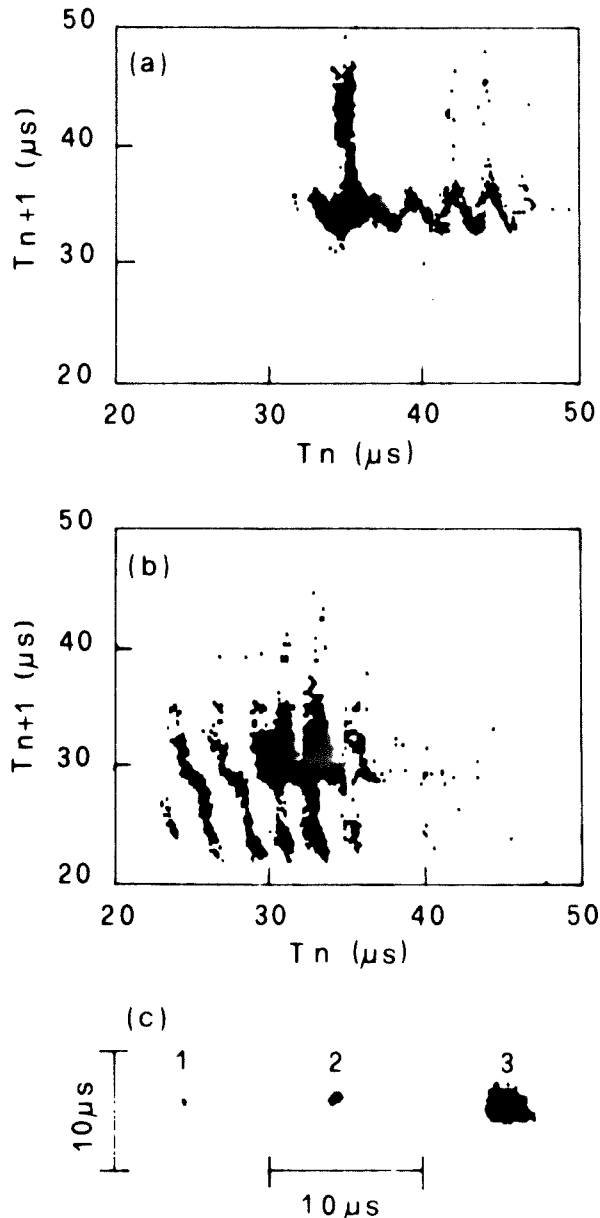


Fig. 6. Experimental return time maps. (a) and (b) refer to the same gain and to B values of 0.459 and 0.427 respectively. (c) shows the maps corresponding to regular periodic situations, namely, (1) an electronic oscillator, (2) the laser in a regular periodic regime and (3) the laser just at the onset of the instability but still with a regular period.

spread has no relevance on the average dynamics, it contributes a large fluctuation enhancement whenever the system slides downhill. In Ref. [18] this was observed in the transient decay of an unstable state, here we report the same feature repeated at each Poincaré cycle.

As a conclusion, low dimensional chaos is described by a small number of coupled deterministic equations [as, e.g., eq (1)], that we write in general as

$$\dot{x}_i = F_i(\{x_j\}) \quad (i, j = 1, 2, 3), \quad (2)$$

where F_i are nonlinear functions whose power expansion implies terms as x_i , x_j and higher order. But whenever this low dimensional chaos is a contracted description of a large system, then x_i are collective variables corresponding to a macroscopic dynamics, and the nonlinearities of eq. (2) depend critically on whether

$$\langle x_i x_j \rangle \simeq \langle x_i \rangle \langle x_j \rangle. \quad (3)$$

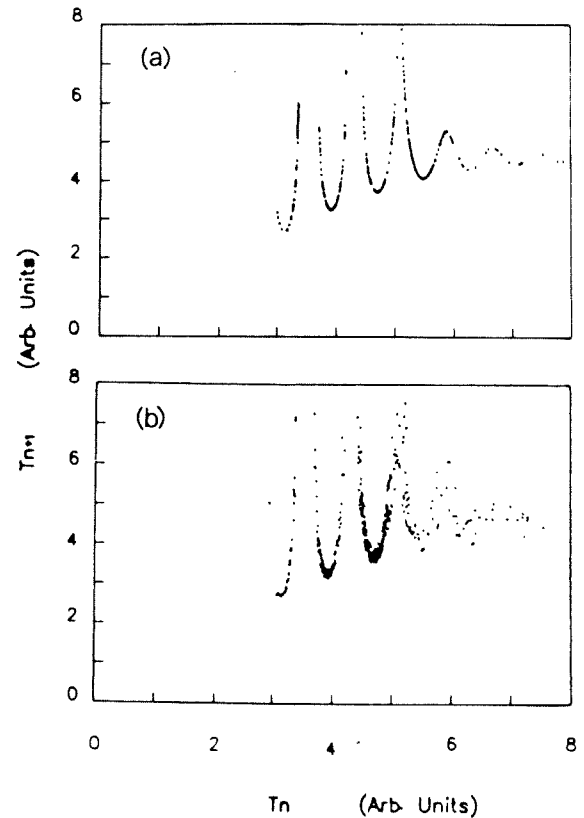


Fig. 7. Numerical return time maps for Shil'nikov chaos. (a) No addition of noise or anharmonic contributions. (b) With the addition of noise (0.4%) and 1% of second and third harmonic contributions.

Relation (3) fails to hold in the decay situations typical of Shil'nikov chaos. In such a case, we have a strong coupling between nonlinear chaotic dynamics and statistical mechanics.

References

1. Lamb, Jr., W. E., Phys. Rev. **134**, A1429 (1964).
2. Haken, H., Laser Theory, in Encyclopedia of Physics, Vol. XXV/2c (Edited by S. Flügge), Springer, Berlin (1970).
3. Scully, M. and Lamb, Jr., W. E., Phys. Rev. Letters **16**, 853 (1966); Phys. Rev. **159**, 208 (1967); **166**, 246 (1968).
4. Gordon, J. P., Phys. Rev. **161**, 367 (1967).
5. Haken, H., Synergetics, 3rd Edn., Springer, Berlin (1983).
6. Arecchi, F. T., Order and Fluctuations in Equilibrium and Nonequilibrium Statistical Mechanics, Proc. XVII Solvay Conf. on Physics (Edited by G. Nicolis *et al.*), J. Wiley, New York (1981).
7. Glauber, R. J., Quantum Optics and Electronics (Edited by C. De Witt *et al.*), Gordon and Breach, New York (1965).
8. Arecchi, F. T., Quantum Optics (Edited by R. J. Glauber), Academic Press, New York (1969).
9. Arecchi, F. T. and Harrison, R. G., (eds.), Instabilities and Chaos in Quantum Optics, Springer Verlag, Berlin (1987).
10. Lorenz, E. M., J. Atmos. Sci. **20**, 130 (1963).
11. Arecchi, F. T., Lippi, G. L., Puccioni, G. P. and Tredicce, J. R., Optics Comm. **51**, 308 (1984).
12. Arecchi, F. T., Meucci, R., Puccioni, G. P. and Tredicce, J. R., Phys. Rev. Lett. **49**, 1217 (1982).
13. Lippi, G. L., Tredicce, J. R., Abraham, N. B. and Arecchi, F. T., Optics Comm. **53**, 129 (1985).
14. Arecchi, F. T., Gadomski, W. and Meucci, R., Phys. Rev. **A43**, 1617 (1986).
15. Arecchi, F. T., Lapucci, A., Meucci, R., Roversi, J. A. and Coulet, P. (to be published).
16. Shilnikov, L. P., D9kl. Akad. Nauk SSSR **160**, 558 (1965); Shilnikov, L. P., Mat. Sbornik **77**, (119) 461 (1968); and **81** (123) 92 (1970).

17. Arnedodo, A., Couillet, P. H., Spiegel, E. A. and Tresser, C., *Physica* **14D**, 327 (1985).
18. (a) Arecchi, F. T., Degiorgio, V. and Querzola, B., *Phys. Rev. Lett.* **19**, 1168 (1967); (b) Haake, F., *Phys. Rev. Lett.* **41**, 1685 (1978); (c) Arecchi, F. T. and Politi, A., *Phys. Rev. Lett.* **45**, 1215 (1980); Arecchi, F. T., Politi, A. and Ulivi, L., *Nuovo Cimento* **71B**, 119 (1982).
19. Arecchi, F. T., Meucci, R. and Gadomski, W., *Phys. Rev. Lett.* **58**, 2205 (1987).
20. Glendinning, P. and Sparrow, C., *Jour. Stat. Phys.* **35**, 645 (1984).
21. Argoul, F., Arneodo, A. and Richetti, P., *Phys. Lett.* **A120**, 269 (1987).